CHORD STRESS EFFECT IN HIGH-STRENGTH STEEL TUBULAR X-JOINTS

SEON-HU KIM[1], CHEOL-HO LEE[2*], and DONG-JIN SHIN[3]

[1]*Department of Architecture & Architectural Engineering, Seoul National University, Seoul 08826, Korea.*
E-mail: rlatjsgn5022@snu.ac.kr
[2]*Department of Architecture & Architectural Engineering, Seoul National University, Seoul 08826, Korea.*
E-mail: ceholee@snu.ac.kr (corresponding author)
[3]*Department of Architecture & Architectural Engineering, Seoul National University, Seoul 08826, Korea.*
E-mail: physicsodor@snu.ac.kr

In tubular structures, chord members can be subjected to substantial axial force or bending moment. Chord sectional stress induced by axial force and bending moment affects static strength of tubular joint. The degree of joint strength degradation caused by chord sectional stress is called chord stress effect. Chord stress effect has generally been investigated through high fidelity finite element (FE) analysis since very complicated experimental setup is often needed to include chord stress effect in testing. Until now, a number of FE studies on chord stress effect have been conducted. However, studies on the chord stress effect of the tubular joints fabricated from high-strength steel are quite limited; a family of constructional steels whose yield stress is higher than 460 MPa is often called high-strength steel. As the material level properties of high-strength steel are significantly different from those of ordinary steel (e.g., lack of yield plateau), high-strength steel joints are expected to exhibit different nonlinear behavior compared to ordinary steel joints. In this study, nonlinear FE analyses were carried out to investigate the behavior of high-strength steel X-joints under the presence of chord stress. High strength steel X-joints made with circular hollow sections (CHSs) and square hollow sections (SHSs) were included in the test-backed numerical analyses. Various chord stress patterns were considered. Overall, the strength decrease due to chord load in high-strength steel joints was shown to be comparable to or less than that of ordinary steel joints. Most of current design standards have imposed some limitations on high-strength steel joints due to concerns about their presumed inferior structural performance. However, from the perspective of chord stress effect, high-strength steel joints generally outperform ordinary steel joints. The validity of the section class limitation on tubular joints, which hampers the use of thin-walled high-strength steel sections, is also questioned.

Keywords: High-strength steel, Tubular structure, X-joint, Chord stress effect, Finite element, Chord stress function.

1 Introduction

The chord stress effect represents the degree of joint strength degradation caused by chord sectional stress. To include chord stress effect chord stress function (Q_f) is used. Chord stress function is defined as the ratio of the joint strength with chord preload to that without chord preload. Chord stress functions for various joint types have been suggested for several decades.

Proceedings of the 17th International Symposium on Tubular Structures.
Editors: X.D. Qian and Y.S. Choo

Published by Research Publishing, Singapore.
ISBN: 978-981-11-0745-0; doi:10.3850/978-981-11-0745-0_050-cd

During codification of its new version of design guide, CIDECT proposed a unified form of chord stress function throughout all joint types. The CIDECT formula for chord stress functions for tubular X-joints (Wardenier et al. 2008, Packer et al. 2009) are shown in **Table 1**. In **Table 1**, CHS and SHS are the abbreviation of circular hollow section and square hollow section, respectively.

Table 1. CIDECT chord stress functions for CHS and SHS X-joints

CHS X-joint		SHS X-joint	
Compressive chord load ($n' < 0$)	Tensile chord load ($n' > 0$)	Compressive chord load ($n' < 0$)	Tensile chord load ($n' > 0$)
$(1-\|n'\|)^{0.45-0.25\beta}$	$(1-\|n'\|)^{0.20}$	$(1-\|n'\|)^{0.6-0.5\beta}$	$(1-\|n'\|)^{0.10}$
Notes: $n' = P/P_y + M/M_p$ (P_y : chord axial yield load, M_p : chord plastic moment). β: brace-to-chord diameter (CHS) or width (SHS) ratio.			

Extensive FE analysis results were used for the formulation of the equations listed in **Table 1**. However, only one steel grade was considered for each X-joint; f_y = 355 MPa for CHS X-joints and f_y = 420 MPa for SHS X-joints (Van der Vegte et al. 2007, Wardenier et al. 2007). The effect of steel grade on the chord stress effect has yet to be well understood. This paper investigates the chord stress effect in the high-strength steel joints and compares it to the ordinary-strength steel joints.

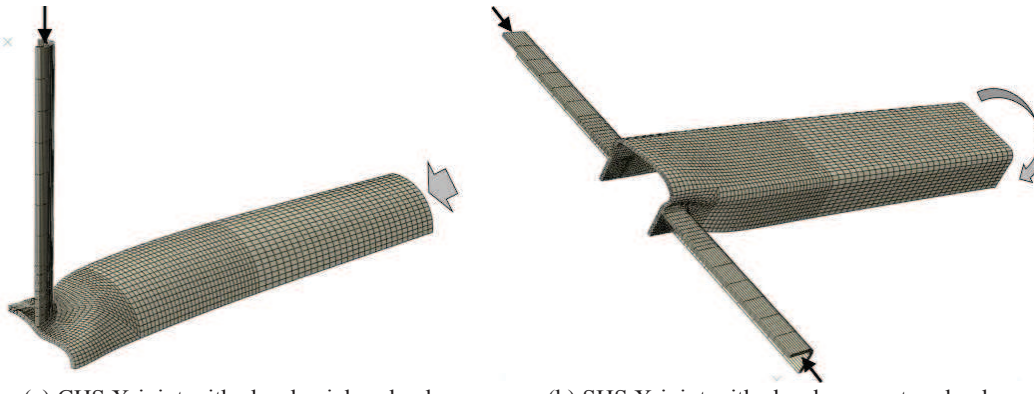

(a) CHS X-joint with chord axial preload (b) SHS X-joint with chord moment preload

Figure 1. Examples of tubular X-joint FE analyses

The authors recently conducted testing on both CHS and SHS X-joints made of HSA800 steel (Lee et al. 2017, Kim et al. 2019). HSA800 is a recently developed high-strength steel in South Korea (f_{yn} = 650 MPa). These experimental and supplemental FE studies clearly indicated that the yield stress upper cap and the strength reduction factors in current standards [e.g. ISO 14346 (ISO 2013)] are unduly conservative for the X type joints and need to be re-examined. In this study, an additional FE analyses were conducted, particularly with focusing on chord stress effect. For the analyses, a general purpose FE code ABAQUS (Simulia 2014) was used. The von Mises yield criterion with isotropic hardening was assumed for the material option and the quadratic solid elements with reduced integration (C3D20R) were used. Examples of the analyzed models are illustrated in **Fig. 1**. Note that as seen in **Fig. 1** reduced joint models (1/4 or 1/8 model) were utilized considering symmetry in geometry and loading. The modeling method

was validated using the results from the aforementioned experiments. For details of the validation readers may refer to Kim and Lee (2018) and Lee et al. (2019).

2 Chord stress effect of tubular X-joints

This section first summarizes general behavioral tendencies of CHS and SHS X-joints under chord stress effect. A measured stress-strain relationship of HSA800 reported in Lee et al. (2017) was employed (f_y = 798 MPa and f_u = 914 MPa).

2.1 *Basic behavior of tubular X-joints without chord load*

Generally, the behavioral pattern of tubular joints under the presence of the chord load is not much deviated from the basic case where chord load is not applied. Thus it is important to understand the basic joint behavior without chord load before investigating the chord stress effect of the X-joints. It is first noted that although CHS and SHS X-joints may appear topologically similar, their nonlinear behavior is significantly different from each other. **Fig. 2** illustrates the yielding pattern of a CHS and an SHS X-joint of similar overall dimensions, at similar indentation level (about 3% of diameter or width). Typically, in CHS X-joints, plastic stress and deformation well develop both at the connecting face and the chord sidewall (chord plastification). In SHS X-joints, however, yielding does not fully spread to the chord sidewall and concentrates at the connecting face and the corner of the chord (chord face plastification). The behavior of SHS X-joints is thus closer to that of a plate subjected to out-of-plane loading.

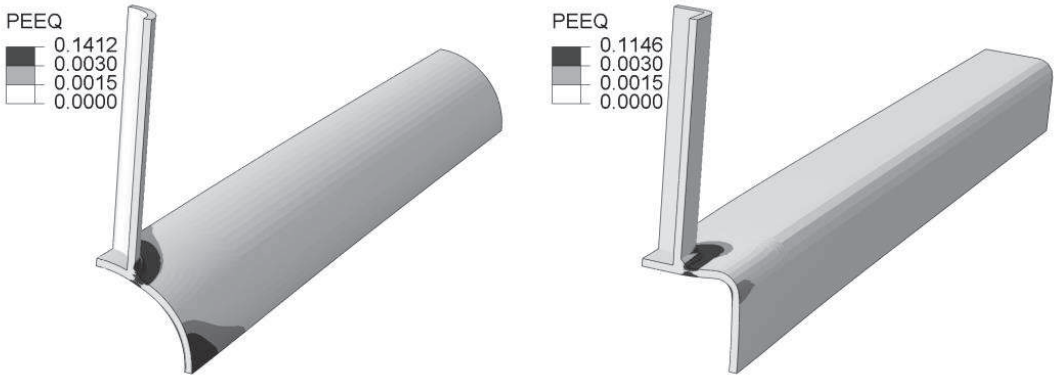

(a) CHS X-joint (b) SHS X-joint

Figure 2. Yield spread pattern (PEEQ plot) of CHS and SHS X-joint without chord load

As a result of different yield mechanism mentioned above, CHS and SHS X-joints exhibit different load-indentation relationship. **Fig. 3** illustrates the load-indentation diagrams of CHS and SHS joints depending on the brace-to-chord diameter (or width) ratio, β. CHS joints undergo strength degradation after reaching the maximum load, while SHS joints generally show a monotonically increasing pattern. The chord plastification mode of CHS joints mobilizes the membrane action of the chord face when β is low. The chord "face" plastification mode of SHS joints tends to be mixed with the chord sidewall buckling as β approaches 1.0. In this study, β values of 0.2, 0.4, 0.62, and 0.8 were considered. The joints with β = 1.0 or close will be considered separately (in future work) as their chord stress effect is significantly different from other joints with moderate β. Note that the 3% deformation criterion (Lu et al. 1994) is adopted throughout this study (the corresponding deformation limit line is provided in **Fig. 3**).

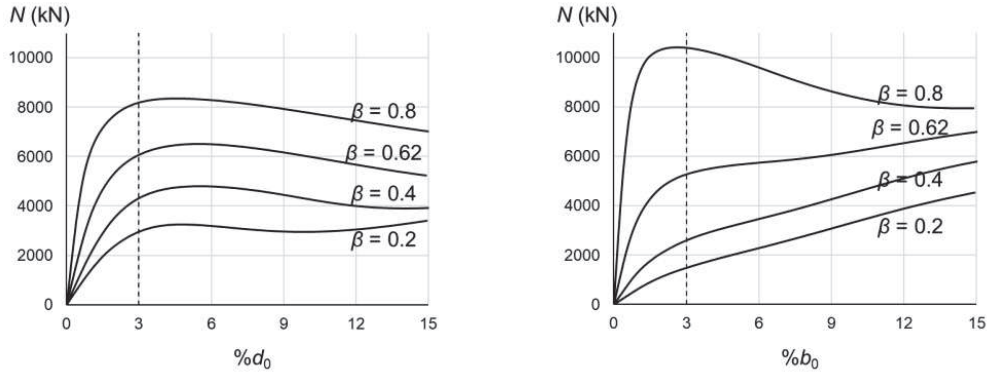

(a) CHS X-joint (b) SHS X-joint

Figure 3. Load-indentation diagrams of tubular X-joint depending on β

2.2 *Chord stress effect considering chord stress patterns*

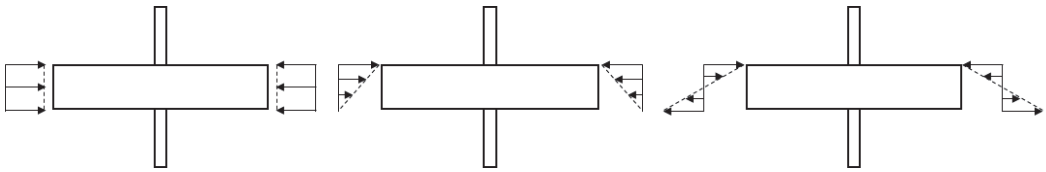

(a) uniform stress (b) triangular stress (c) moment gradient stress

Figure 4. Representative chord stress patterns

Three representative chord stress patterns were considered in the FE analyses: uniform stress, triangular stress, and moment gradient stress (**Fig. 4**). Uniform stress and moment gradient stress can be obtained by applying axial load and bending moment to the chord ends, respectively. Triangular stress can be achieved by properly applying combined axial load and bending moment. The influence of these chord stresses on the joint behavior is shown in **Fig. 5**. In **Fig 5**, 'M' stands for the moment gradient stress pattern, and 'C' and 'T' represent compressive and tensile load, respectively. The solid lines indicate the case with no chord load. All dashed lines correspond to chord stress level (n) of ±0.6; here, chord stress level is defined as the ratio of the maximum stress at extreme fiber (chord connecting face) to the chord yield stress ($n > 0$ for tensile stress). Note that n is similar but not equal to n' in **Table 1**. It is observed in **Fig. 5** that compressive stress has more adverse effect on the joint behavior compared with tensile stress. Tensile stress can be either detrimental or beneficial depending on the joint geometry. The moment stress case ('M') involves both compressive and tensile stress, however, is much closer to the compressive case ('C'). In both CHS and SHS X-joint, the joint behavior becomes more sensitive to the stress profile when β is higher. The joints with higher β transfer more load into the chord sidewall, and thus, they are more affected by the chord stress at the sidewall. Since the main difference among the three stress patterns in **Fig. 4** is the stress state at the sidewall, the high sensitivity to the stress patterns observed in the joints with high β can be explained.

The CIDECT formula for chord stress function (**Table 1**) covers the effect of different stress patterns by using n' (= $P/P_y + M/M_p$) instead of n in its formulation. For a chord stress

level (n), n' differs depending on stress pattern; n' is higher when chord axial load is applied, compared to when chord is subjected to bending moment. The CIDECT formula is highly efficient from the perspective that the effect of chord stress pattern is condensed into a single term n'; however, in turn, taking this simple form has compromised physical significance.

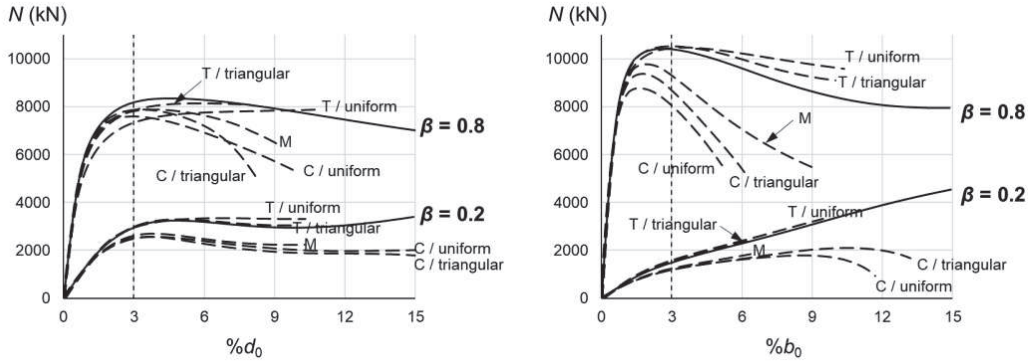

(a) CHS X-joint (b) SHS X-joint

Figure 5. Chord stress effect in tubular X-joints

3 Comparison of chord stress effect between ordinary- and high-strength steel joints

Extensive FE analyses were conducted to compare the chord stress effect in ordinary-strength steel joints and high-strength steel joints. The parameters considered in the analyses are summarized in **Table 2**. One ordinary-strength steel (SM490) and one high-strength steel (HSA800) were included. Note that even in the most generous design standard for tubular joints, the maximum allowable yield stress is 700 MPa (CEN 2007); HSA800 steel in **Table 2** (f_y = 798 MPa) is beyond the limit. All possible combinations of the parameters in **Table 2** were tried. The results from the numerical analyses are evaluated using the CIDECT formula in **Fig. 6**. Overall, the chord stress function (Q_f) of the high-strength steel joints is higher than that of the ordinary-strength steel joints. HSA800 joints are particularly superior to SM490 joints when n' is high ($|n'| \rightarrow 1.0$). When each of them is compared to the corresponding SM490 joint, HSA800 joints showed chord stress function 6% and 3% higher in average for CHS X and SHS X type, respectively. **Fig. 6** shows that the current CIDECT formula for chord stress function is extrapolatable to high-strength steel whose yield stress is as high as 800 MPa.

Table 2. Parameters used in FE analyses

Parameter	Values used
Steel grade	SM490[a] (f_y = 324 MPa, f_u = 518 MPa) and HSA800[a] (f_y = 798 MPa, f_u = 914 MPa)
β (brace-to-chord diameter/width[b] ratio)	0.2, 0.4, 0.62, and 0.8
2γ (chord diameter/width[b]-to-thickness ratio)	20, 26, and 40
n (chord stress level)	-0.9, -0.6, -0.3, 0, 0.3, 0.6, and 0.9
Chord stress pattern (see **Fig. 4**)	Uniform, triangular, and moment stress
[a] Measured stress-strain property reported in Lee et al. (2017) was used. [b] Diameter for CHS X-joint and width for SHS X-joint.	

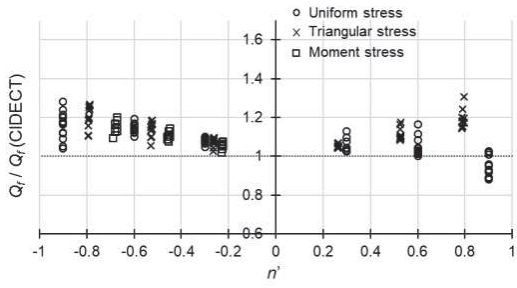

(a) CHS X-joint, SM490

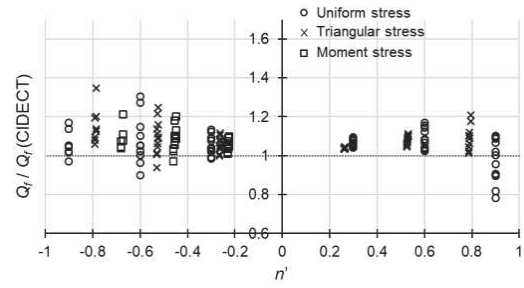

(b) SHS X-joint, SM490

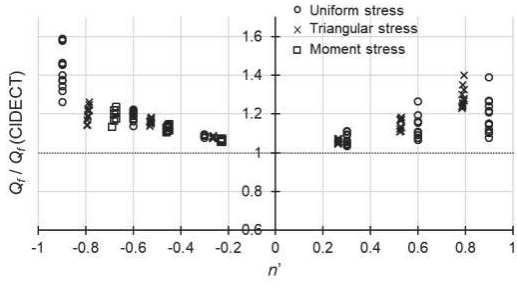

(a) CHS X-joint, HSA800

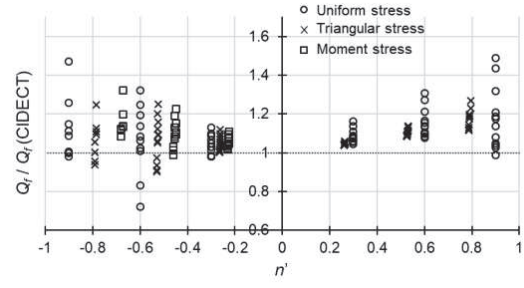

(b) SHS X-joint, HSA800

Figure 6. Evaluation of chord stress function of tubular X-joints

Not only the upper limit imposed on the yield stress, but also the limitation regarding section slenderness acts as a barrier to the use of high-strength steel to tubular joints. According to the current CIDECT recommendation, the section class of the chord is limited to the Eurocode Class 1 and 2 (CEN 2005). Class 1 and 2 cross sections are those which can develop their plastic moment resistance. **Table 3** summarizes the Eurocode section class limits for SM490 and HSA800 steel used in this study, in terms of 2γ, the chord diameter/width-to-thickness ratio. It is noted that each joint model in the FE analyses had 2γ value of 20, 26, or 40 (**Table 2**). All SM490 joints meet the Class 2 requirement, or just slightly violate it. On the other hand, for the HSA800 joints, CHS joints with 2γ = 26 or 40 and SHS joints with 2γ = 40 do not satisfy the Class 2 requirement; moreover, SHS joints with 2γ = 40 is even more slender than Class 3. In principle, these joints with Class 3 or 4 chord section cannot be designed, or may be designed by replacing M_p with the nominal moment capacity corresponding to the class (for example, M_y for Class 3) when calculating the "chord demand level" n' (= $P/P_y + M/M_p$, see **Table 1**). In **Fig. 6**, however, all the joints were evaluated without considering these aspects regarding section slenderness. Hence, the satisfactory performance of HSA800 joints shown in **Fig. 6** implies that the class of the chord cross-section may be somewhat relaxed. This is well explained if the joint indentation is deemed as a huge geometric imperfection or local buckling boundary. It is speculated that compressive load in the chord member is unlikely to develop another local buckling which would affect the joint strength. For high-strength steel tubular X-joints, the section class limitation in design standard needs further investigation.

Table 3. Eurocode section class limits

Steel grade	SM490	HSA800

f_y (MPa)	324	798
Class 1&2 limit (CHS)	$2\gamma < 50.8$	$2\gamma < 20.6$
Class 3 limit (CHS)	$2\gamma < 65.3$	$2\gamma < 26.5$
Class 1&2 limit (SHS)	$2\gamma < 38.4$	$2\gamma < 26.6$
Class 3 limit (SHS)	$2\gamma < 41.8$	$2\gamma < 28.8$
Notes; 2γ: chord diameter/width-to-thickness ratio. Corner outer radius of the chord was three times the chord thickness for all SHS joint models, and this was considered in preparing the limit values of SHS.		

4 Summary and conclusions

The nonlinear behavior of high-strength steel tubular X-joints under the presence of chord preload was investigated. Test-validated numerical analyses were conducted on CHS and SHS X-joints subjected to brace axial compression. Following conclusions can be drawn.

(i) Since the basic nonlinear behavior of tubular X-joint is highly dependent on the chord section type (circular vs. square) and the brace-to-chord diameter/width ratio, the way the chord load affects the joint behavior is also sensitive to these geometric factors.
(ii) Not only the magnitude but also the pattern of the chord stress affects the chord stress effect. The chord stress pattern becomes more influential when the brace becomes larger relative to the chord
(iii) The high-strength steel X-joints analyzed in this study, whose yield stress is as high as 800 MPa, generally outperformed ordinary-strength steel joints in terms of chord stress effect.
(iv) The section class limitation in current design standard was shown to be too stringent for high-strength steel X-joints and needs more detailed investigation.

Acknowledgments

This study was supported by a grant from the POSCO Affiliated Research Professor Program.

References

CEN (European Committee for Standardization), *Design of Steel Structures (Eurocode No. 3) - Part 1.1: General Rules and Rules for Buildings*, Brussels, Belgium, 2005.

CEN (European Committee for Standardization), *Design of Steel Structures (Eurocode No. 3) - Part 1.12: Additional Rules for the Extension of EN 1993 up to Steel Grades S700*, Brussels, Belgium, 2007.

ISO (International Organization of Standardization), *Static design procedure for welded hollow-section joints – Recommendations*; *ISO/FDIS 14346:2012(E)*, 2013.

Kim, S.-H. and Lee, C.-H., Structural Performance of CHS X- Joints Fabricated From High- Strength Steel, *Steel Construction*, 11(4), 278-285, 2018.

Kim, J.H., Lee, C.H., Kim, S.H., and Han, K.H., Experimental and Analytical Study of High-strength Steel RHS X-joints under Axial Compression, *ASCE J. of Structural Engineering*, accepted in 2019.

Lee, C.-H., Kim, S.-H., Chung, D.-H., Kim, D.-K., and Kim, J.-W., Experimental and numerical study of cold-formed high-strength steel CHS X-joints. *ASCE J. of Structural Engineering*, 143(8): 04017077, 2017.

Lee, C.-H., Kim, S.-H., and Kim, J.-H., Behavior of RHS X-joints Having High Brace to Chord Width Ratio under Axial Compression, in *The Seventh International Conference on Structural Engineering, Mechanics and Computation* (will be held in September 2019 at Cape Town, South Africa), accepted in 2019.

Lu, L., De Windel, G., Yu, Y., and Wardenier, J., Deformation Limit for the Ultimate Strength of Hollow Section Joints, in *Sixth International Symposium on Tubular Structures*, 1994.

Packer, J. A., Wardenier, J., Zhao, X. L., van der Vegte, G. J., and Kurobane, Y., *Construction with Hollow Steel Sections – No. 3: Design Guide for Rectangular Hollow Section (RHS) Joints under Predominantly Static Loading*, 2nd ed, CIDECT, Geneva, Switzerland, 2009.

Simulia, *Abaqus 6.14: Abaqus/CAE User's Guide*, Providence, RI, 2014.

Van der Vegte, G. J., Wardenier, J., and Makino, Y., Effect of Chord Load on Ultimate Strength of CHS X-Joints, *Int. J. Offshore and Polar Engineering*, 17(4), 301-308, 2007.

Wardenier, J., Van der Vegte, G. J., and Liu, D. K., Chord Stress Function for Rectangular Hollow Section X and T joints, in *Seventeenth International Offshore and Polar Engineering Conference*, 2007.

Wardenier, J., Kurobane, Y., Packer, J. A., Van der Vegte, G. J., and Zhao, X. L., *Construction with Hollow Steel Sections – No. 1: Design Guide for Circular Hollow Section (CHS) Joints under Predominantly Static Loading*, 2nd ed., CIDECT, Geneva, Switzerland, 2008.